Published in final edited form as:
Invest Ophthalmol Vis Sci. 2008 September ; 49(9): 3961–3969. doi:10.1167/iovs.08-1915.

Cultured Porcine Trabecular Meshwork Cells Display Altered Lysosomal Function When Subjected to Chronic Oxidative Stress

Paloma B. Liton, **Yizhi Lin**, **Coralia Luna**, **Guorong Li**, **Pedro Gonzalez**, and **David L. Epstein**
Department of Ophthalmology, Duke University Eye Center, Durham, North Carolina

Abstract

Purpose—To investigate the effects of chronic oxidative stress on lysosomal function in trabecular meshwork (TM) cells.

Methods—Confluent cultures of porcine TM cells were grown for 2 weeks in physiological (5% O_2) or hyperoxic conditions (40% O_2) in the presence or absence of the protease inhibitor leupeptin (10 μM). The following parameters were quantified using the fluorogenic probes indicated within parentheses: autofluorescence, intracellular reactive oxygen species (ROS; H_2DCFDA), mitochondrial membrane potential (JC-1), mitochondrial content (Mitotracker Red; Invitrogen-Molecular Probes, Eugene, OR), lysosomal content (acridine orange and Lysotracker Red [Invitrogen-Molecular Probes]), autophagic vacuole content (MDC), SA-β-galactosidase (FDG), and cathepsin activities (z-FR-AMC). Cathepsin levels were quantified by qPCR and Western blot analysis. Ultrastructural analysis was performed by transmission electron microscopy.

Results—Prolonged exposure of porcine TM cells to a hyperoxic environment led to an increase in ROS production and oxidized material. Electron micrographs revealed the cytoplasmic accumulation of lipofuscin-loaded lysosomes. Augmented lysosomal and autophagic vacuole content was confirmed with specific fluorophores. The mRNA and protein levels of several cathepsins were upregulated with oxidative stress. This up-regulated expression did not correlate with increased lysosomal activity.

Conclusions—The results indicate that chronic exposure of TM cells to oxidative stress causes the accumulation of nondegradable material within the lysosomal compartment, leading to diminished lysosomal activity. Since the lysosomal system is responsible for the continuous turnover of cellular organelles, impaired lysosomal activity may lead to progressive failure of cellular TM function with age.

Glaucomas comprise a group of eye diseases that ultimately lead to optic nerve damage and consequent irreversible blindness. Although the specific cause of most forms of the disease has not yet been determined, aging of the trabecular meshwork (TM), the tissue responsible for maintaining proper levels of intraocular pressure (IOP), is suspected to be a major risk factor in the development or progression of the most common form of the disease, primary open-angle glaucoma (POAG).[1]

Corresponding author: Paloma B. Liton, Duke University Eye Center, Erwin Road, Box 3802, Durham, NC 27710; paloma.liton@duke.edu.

Disclosure: **P.B. Liton**, None; **Y. Lin**, None; **C. Luna**, None; **G. Li**, None; **P. Gonzalez**, None; **D.L. Epstein**, None

Aging is a complex phenomenon associated with a progressive accumulation of deleterious changes that results in a gradual decline in cellular and physiological function, as well as a diminished capacity to respond to stress, thus increasing the probability of degenerative disease.[2] A free radical theory of aging has been proposed, connecting the oxidative environment and aging process.[3] According to this theory, reactive oxygen species (ROS) resulting from normal aerobic metabolism are responsible for continuous macromolecular damage. Although most damaged biomolecules and organelles are successfully removed by the cellular proteolytic systems, the recycling machinery is inherently imperfect and is affected by the aging process. Thus, many types of cells and tissues accumulate oxidatively damaged material during aging and age-related disorders. A slow accumulation and age-associated accumulation of materials that cannot be degraded primarily occurs in long-lived postmitotic or terminally differentiated cells such as TM cells, leading to the build-up of considerable amounts of waste material.[4,5] The validity of the free radical theory of aging has been extensively supported by numerous in vivo and in vitro studies showing that age-related changes accelerate under the influence of oxidative stress, whereas various antioxidants slow aging.[6–8]

Several groups have reported increased expression of oxidative markers, such as oxidative DNA damage and peroxidized lipids, as well as diminished antioxidant potential in the TM tissue of donors with glaucoma, supporting a key role of oxidative stress in the morphologic and physiological alterations observed in the outflow pathway tissue in aging and POAG.[9–11] In addition, we have recently demonstrated an increased number of cells with abnormal β-galactosidase activity at pH 6 (SA-β-gal) in the glaucomatous outflow pathway.[12] Although the nature of such activity remains unknown, SA-β-gal has been proposed to be a manifestation of residual lysosomal β-galactosidase activity at a suboptimal pH that becomes detectable due to the increased lysosomal content in aged cells.[13–15] The lysosomal compartment is the terminal degradative compartment responsible for the turnover of long-lived proteins and “worn out” organelles. Probably because of such disposal function, lysosomes are the major proteolytic system affected by age.[16–19] Alterations of lysosomal function have been implicated in the pathogenesis of several age-related disorders.[20–26]

The purposes of this study were to evaluate hyperoxia as an in vitro model for studying the molecular mechanisms underlying aging of postmitotic TM cells and to examine the effect of chronic oxidative stress/aging in the TM lysosomal system. The data presented provide evidence of impaired lysosomal function as a result of the accumulation of biological debris in aged/oxidized TM cells.

Material and Methods

Generation of Primary Cultures of Porcine TM Cells

Primary cultures of porcine TM cells were prepared from porcine eyes obtained from a local abattoir less than 5 hours postmortem. Briefly, the TM was dissected and digested with 2 mg/mL of collagenase for 1 hour at 37°C. The digested tissue was placed in gelatin-coated 35-mm dishes and cultivated in low-glucose Dulbecco’s modified Eagle’s medium (DMEM) with L-glutamine and 110 mg/L sodium pyruvate, supplemented with 10% fetal bovine serum (FBS), 100 mM nonessential amino acids, 100 U/mL penicillin, 100 mg/mL streptomycin sulfate, and 0.25 mg/mL amphotericin B; all the reagents were obtained from Invitrogen (Carlsbad, CA). Cells were maintained and propagated until passage 3 at 37°C in humidified air with 5% CO_2. Cell lines were subcultivated 1:2 when confluent. Up to six different cell lines were used in the present study.

Experimental Model of Chronic Oxidative Stress in Porcine TM Cells

Chronic oxidative stress was induced by subjecting porcine TM cells to normobaric hyperoxia conditions. Confluent cultures of porcine TM cells at passage 4 were grown for 2 weeks at 40% O_2 and 5% CO_2. Control cultures were grown under physiological oxygen conditions (5% O_2, 5% CO_2) in a triple-gas incubator. To suppress lysosomal proteolysis, the thiol protease inhibitor leupeptin (Sigma-Aldrich, St. Louis, MO) was added to the medium twice per week at a concentration of 10 μM.[27]

Measurement of Cell Size

After the stress period, cells were trypsinized and subcultivated at low density. After 1 day, when the cells had attached, images were obtained in randomly selected fields, and the area of 25 randomly selected cells from each group was measured (Photoshop; Adobe Systems, San Diego, CA) by outlining the cell area (Magnetic Lasso Tool; Adobe Systems) and using the histogram function to count pixels in those areas.

Measurement of Endogenous Cellular Autofluorescence

Endogenous cellular autofluorescence was detected under the FITC filter by fluorescence microscopy and quantified by flow cytometry (FACSCalibur; BD Biosciences, San Jose, CA). For this, the fluorescence emitted by 10,000 cells in the FL-2 channel (563– 607 nm wavelength band) was recorded and analyzed (CellQuest software; BD Biosciences).

Cell Viability and Proliferation

Cell viability was quantified by trypan blue exclusion staining. Cell proliferation after a period of stress was quantified with a BrdU cell proliferation assay (Calbiochem, San Diego, CA) according to the manufacturer's instructions.

Quantification of Intracellular ROS Production

Intracellular ROS production was quantified with the cell-permeant ROS indicator 2′,7′-dichlorodihydrofluorescein diacetate (H_2DCFDA, Invitrogen). Briefly, the cells (1×10^6) were trypsinized and incubated in 1 mL PBS containing 20 μM H_2DCFDA for 30 minutes. After this loading period, the cells were washed, and the mean green fluorescence of 10,000 cells was immediately recorded and quantified by flow cytometry and the system software (FL-1 channel; CellQuest; BD Biosciences). Nonstained control cells were included to evaluate baseline fluorescence. The laser intensity settings were adjusted to the lowest level at which autofluorescence was not detected.

Measurement of Mitochondrial Membrane Potential

The integrity of the mitochondrial membrane (Ψm) was evaluated with the cationic dye JC-1 (Invitrogen). Cells (1×10^6) were trypsinized and incubated at 37°C for 30 minutes in 1 mL complete medium containing 2 μM JC-1. The cells were washed and the mean green fluorescence (FL-1 channel) and mean orange-red fluorescence (FL-2 channel) were recorded and quantified by flow cytometry (CellQuest software; BD Biosciences). Ψm was expressed as the mean red to mean green ratio. Nonstained control cells were included to evaluate baseline fluorescence. The laser intensity setting used in these experiments was not strong enough to excite at the autofluorescence level.

Quantification of DNA Damage

DNA fragmentation associated with oxidative DNA damage was analyzed by a single-cell gel electrophoresis assay (Comet Assay Kit; Trevigen, Gaithersburg, MD) according to manufacturer's instructions. Electrophoresis was performed by using the alkaline

electrophoresis protocol to detect single-stranded DNA breaks, double-stranded DNA breaks, and apurinic and apyrimidinic sites, as well as alkali-labile DNA adducts. The comet length of 50 randomly selected cells from each group was quantified by a masked observer using the comet scoring software (Comet Score; TriTek Corp., Summerduck, VA).

Protein Carbonylation Assay

The detection of carbonyl groups introduced into proteins by oxidative reaction was performed with a protein oxidation kit (Oxyblot; Chemicon, Temecula, CA) according to the manufacturer's instructions.

Electron Microscopy

The cells were washed twice in PBS and fixed in 2.5% glutaraldehyde in 0.1 M cacodylate buffer (pH 7.2). Fixed cells were then detached by gentle scraping, pelleted, postfixed in 1% osmium tetroxide in 0.1 M cacodylate buffer and processed for transmission electron microscopy in the Morphology Facility at Duke University Eye Center. Thin sections (65 nm) were examined by electron microscopy (JEM-1200EX; JEOL USA, Peabody, MA).

Quantification of Lysosomal and Mitochondrial Cellular Content

The lysosomal cellular content was evaluated using lysosomotropic dyes (Lysotracker Red [LTR]; Invitrogen) and acridine orange (AO; Sigma-Aldrich) as follows. The cells were incubated for 15 minutes at 37°C in fresh culture medium containing either LTR (500 nM) or AO (5 μg/mL). Specific lysosomal labeling was confirmed by fluorescence microscopy and quantified by flow cytometry in the red spectrum (FL-3 channel). For evaluation of the mitochondrial cellular content, a red fluorescent dye (MitoTracker Red [MTR] 500 nM; Invitrogen-Molecular Probes, Eugene, OR) was used instead.

Quantification of Autophagic Vacuoles

The autophagic vacuole (AV) content was quantified with the specific dye monodansylcadaverine (MDC; Sigma-Aldrich), as described elsewhere.[28] Briefly, cells grown in 24-well plates were incubated for 15 minutes at 37°C with MDC (0.1 mM) in fresh culture medium. The cells were then extensively washed with PBS and lysated in 10 mM Tris-HCl (pH 8) containing 0.1% Triton X-100. Intracellular MDC was quantified by using a microtiter plate reader (excitation [exc]: 380 nm; emission [em]: 530 nm). To normalize the measurements to the number of cells present in each well, we added a solution of ethidium bromide to a final concentration of 0.2 μM, and the DNA fluorescence was measured (exc: 530 nm, em: 590 nm).

Flow Cytometry Determination of SA-β-gal Activity

Quantification of SA-β-gal activity was performed by flow cytometry with the fluorogenic substrate C_{12}FDG (Invitrogen). First, alkalinization of the lysosomal compartment was induced by treating cell mono-layers with 300 μM chloroquine for 1 hour at 37°C under 5% CO_2. The cells (1×10^6) were then trypsinized and incubated for 1 minute at 37°C in 50 μL of prewarmed PBS containing C_{12}FDG (33 μM). C_{12}FDG uptake was stopped by adding 500 μL ice-cold PBS. The mean green fluorescence of 10,000 cells was recorded (FL-1 channel) 30 minutes later and quantified (CellQuest software; BD Biosciences). Nonstained control cells were included, to evaluate the baseline fluorescence. The laser intensity settings were adjusted to the lowest level so as not to detect autofluorescence.

Quantitative Real-Time PCR

Total RNA from porcine TM primary cultures was isolated (RNeasy kit; Qiagen, Valencia, CA) according to the manufacturer's protocol and treated with DNase. RNA yields were

determined with a green fluorescent dye (RiboGreen; Invitrogen-Molecular Probes). First-strand cDNA was synthesized from total RNA (1 μg) by reverse transcription using oligo(dT) primer and reverse transcriptase (Superscript II; Invitrogen). Real-time PCR was performed in a 20-μL mixture containing 1 μL of the cDNA preparation diluted five times, 10 μL master mix (iQ SYBR Green Supermix; Bio-Rad, Hercules, CA), and 500 nm of each primer in a thermocycler system (iCycler iQ; Bio-Rad) using the following PCR parameters: 95°C for 5 minutes, followed by 50 cycles of 95°C for 15 seconds, 60°C for 15 seconds, and 72°C for 15 seconds. The fluorescence threshold value (Ct) was calculated using the thermocycler system software. The absence of nonspecific products was confirmed by both the analysis of the melt curves and by electrophoresis in 3% acrylagarose gels. β-Actin served as an internal standard of mRNA expression. The change (x-fold) was calculated with the formula $2^{-\Delta\Delta Ct}$, where $\Delta Ct = Ct_{\text{gene}} - Ct_{\text{Act}}$, and $\Delta\Delta Ct = \Delta Ct_{\text{Exp}} - \Delta Ct_{\text{Con}}$. The sequences of the primers used for the amplifications are shown in Table 1.

Western Blot Analysis

Cells were washed twice in PBS and lysated in 20 mM HEPES, 2 mM EGTA, 5 mM EDTA, and 0.5% NP-40 containing protease inhibitor cocktail and phosphatase inhibitor cocktail (Halt; Pierce Biotechnology, Rockford, IL). After sonication for 1 minute on ice, the lysates were clarified by centrifugation, and protein concentration was determined with a protein assay kit (Micro BCA; Pierce Biotechnology). Protein samples (20 μg) were separated by 10% SDS-PAGE and transferred to PVDF membranes (Bio-Rad). The membranes were blocked with 5% nonfat dry milk and incubated overnight with anti-cathepsins (SC-6499), anti-cathepsin K (SC-6506), or anti-tubulin (SC-9935) from Santa Cruz Biotechnology (Santa Cruz, CA). The bands were detected by incubation with a secondary antibody conjugated to horseradish peroxidase and chemiluminescence substrate (ECL Plus; GE Healthcare, Pittsburgh, PA).

Assessment of Lysosomal Enzyme Activity

Cells grown in a 24-well plate were washed in PBS and lysated for 30 minutes at 4°C with shaking in 100 μL of 50 mM sodium acetate (pH 5.5), 2.5 mM DTT, 2.5 mM EDTA, and 1% Triton X-100. The lysates were clarified by centrifugation and immediately used for determination of proteolytic activity. For this, 5 μL of lysates was incubated at 37°C for 30 minutes in lysis buffer (100 μL) in the presence of the omnicathepsin fluorogenic substrate z-FR-AMC (20 μM; Santa Cruz Biotechnology). The AMC released as a result of proteolytic activity was quantified with a microtiter plate reader (exc: 380 nm; em: 440 nm), and normalized by total protein content. Cathepsin protein levels were also analyzed by immunoblot.

Statistic Analysis

All experimental procedures were repeated at least three times in independent experiments with different cell lines. The percentage of increase of the experimental conditions compared with the control was calculated and averaged. Data are represented as the mean ± SD and were analyzed with Student's t-test. $P < 5\%$ was considered statistically significant.

Results

Hyperoxia as an Experimental Model of Aging in Porcine TM Cells

To reproduce the effects of chronic oxidative stress in postmitotic porcine TM cells in vitro, we chose the normobaric hyperoxia model, which consists of growing the experimental cultures in 40% O_2. Control cultures were grown in physiological (5%) O_2.[29] To accelerate the amount of nondegradable oxidized material that might accumulate in vivo during a

lifetime, the cultures were supplemented twice per week with the lysosomal protease inhibitor leupeptin (10 μM).[27] All cultures remained confluent, and cell viability was not affected under any conditions (Supplementary Fig. S1A, http://www.iovs.org/cgi/content/full/49/9/3961/DC1). Cultures grown at 40% O_2 demonstrated a significant decrease in the proliferation rate (55.33% ± 10.98%, $P = 0.0009$, $n = 3$; Supplementary Fig. S1B). In addition, cells grown in 40% O_2 displayed a morphology characterized by enlarged size (24,973 ± 9,242 pixels versus 68,740 ± 17,065 pixels, $n = 20$, $P < 0.0003$) and the accumulation of autofluorescence granules in the perinuclear region (Fig. 1).

Effect of Hyperoxia on Intracellular ROS Production and Ψm in Porcine TM Cells

Cells incubated at 40% oxygen showed a significant increase (104.42% ± 50.85%, $P = 0.026$, $n = 3$) in ROS production compared with physiological conditions (Fig. 2A). This increase in ROS production was accompanied by a statistically significant decrease in the Ψm (27.86% ± 4.11%, $P = 0.007$, $n = 3$; Fig. 2B). The labeling of the cells with a cell-permeant dye (Mitotracker Red; Invitrogen-Molecular Probes) that accumulates within the mitochondria independently of the Ψm, demonstrated augmented mitochondrial content under oxidative stress conditions (96.94% ± 21.69%, $P = 0.008$, $n = 3$; Fig. 2C). These data suggest the accumulation of defective mitochondria in the cells cultured at higher oxygen concentrations. Leupeptin did not have any significant synergistic effect. In addition, cultures of porcine TM cells at 40% O_2 demonstrated increased DNA damage (27.73% ± 9.23%, $P = 0.04$, $n = 3$) as well as elevated protein carbonyl content (Supplementary Fig. S2, http://www.iovs/org/cgi/content/full/49/9/3961/DC1).

Accumulation of Lipofuscin-Loaded Lysosomes in Porcine TM Cells Exposed to Hyperoxic Conditions

As shown in Figure 2D, the incubation of TM cells at 40% O_2 significantly increased the presence of intracellular cross-linked oxidized material (lipofuscin autofluorescence; 156.24% ± 85.85%, $P = 0.035$, $n = 3$). Moreover, electron micrographs from porcine TM cells demonstrated the cytoplasmic accumulation of membrane-bound organelles in the perinuclear region in the cultures exposed to 40% O_2. These vesicles were higher in quantity and larger in size (> 500 nm) than the ones observed under 5% O_2 conditions (≈200 nm, primary lysosomes). In addition, they contained amorphous electron-dense material and membranous structures, phenotypic features characteristic of autophagic secondary lysosomes (Fig. 3). Leupeptin treatment slightly increased the levels of autofluorescence (38.35% ± 10.80%, $P = 0.005$, $n = 3$) as well as the number of such cytoplasmic figures.

Effect of Chronic Oxidative Stress on the Lysosomal Cellular Content in Cultured Porcine TM Cells

The lysosomal compartment is the final destination of the degradative cellular mechanism. To test the capacity of TM cells to respond to the increased intracellular levels of nondegradable material by enhancing the synthesis of novel lysosomes, we measured the total lysosomal cellular content with a lysosomotropic dye (LTR; Invitrogen) and AO. Figure 4A shows a representative experiment of porcine TM cells labeled with LTR, demonstrating a red cytoplasmic punctuate staining in the perinuclear region, corresponding to the subcellular localization of lysosomes. Quantification of the fluorescence intensity per individual cell showed a dramatic increase (323.90% ± 88.30%, $P = 0.005$, $n = 4$) in the lysosomal content in cells exposed to an oxidative environment (Fig. 4B). Similar results, although to a lesser degree, were observed using AO (75.33% ± 36.98%, $P = 0.026$, $n = 4$; Fig. 4C). Cultures treated with leupeptin also showed a significant increase in lysosomal content (LTR: 61.53% ± 32.17%, $P = 0.031$, $n = 4$; AO: 27.72% ± 15.02%, $P = 0.03$, $n = 4$). No synergistic effect was found between proteolysis inhibition and oxidative stress.

Increased Autophagic Vacuoles Content in Cultured Porcine TM Cells Exposed to Chronic Oxidative Stress

The oxidized material is delivered to the lysosomal compartments through autophagy, a process that involves the formation of the so-called autophagic vacuole (AV). As shown in Figure 5, cell cultures grown at 40% O_2 demonstrated an increased AV content (30.74 ± 25.08, $P = 0.03$, $n = 6$). The effect was more pronounced if cells were cultivated in combination with the lysosomal inhibitor leupeptin (51.29% ± 33.05%, $P = 0.01$, $n = 6$).

Effect of Chronic Oxidative Stress on Lysosomal Function in Cultured Porcine TM Cells

We recently reported an increased number of cells positively stained for abnormal SA-β-gal activity in the glaucomatous outflow pathway.[12] Accumulation of nondegradable material in autophagic secondary lysosomes has been proposed to result in increased lysosomal mass and increased lysosomal enzyme content, which manifests in detectable β-galactosidase activity at abnormal pH 6.0.[13–15] As shown in Figure 6A, incubation of TM cells at 40% oxygen atmosphere significantly induced β-galactosidase activity at pH 6.0 (109.9% ± 43.1%, $P = 0.01$, $n = 3$). This effect was not due to increased expression of the β-galactosidase gene (Fig. 6B, GLB-Lys). Of interest, leupeptin treatment induced per se the appearance of this abnormal SA-β-gal activity (47.59% ± 28.85%, $P = 0.04$, $n = 3$) and showed a synergistic effect in conjunction with hyperoxic conditions (197.63% ± 40.34%, $P = 0.002$, $n = 3$).

Quantitative real-time PCR analysis demonstrated the up-regulation with oxidative stress of LAMP2, involved in the transport of proteins into lysosomes, as well as several lysosomal enzymes, in particular cathepsin K (6.86 ± 2.22-fold, $P = 0.032$, $n = 3$; Fig. 6B), The mRNA levels for this protein dramatically increased when cells were cultivated under 40% O_2 in the presence of leupeptin (18.06 ± 2.37-fold, $P = 0.005$, $n = 3$). Western blot analysis using a generic antibody against cathepsins confirmed elevated intracellular levels of cathepsin proteins in the leupeptin-treated and oxidatively stressed cultures (Fig. 6C). The specific antibody against cathepsin K showed increased protein levels of cathepsin K in the leupeptin-treated cultures (5% and 40% O_2); however, no significant effect of oxidative stress on the protein content for this particular cathepsin was found, despite the observed upregulated expression at the mRNA level. It has been described that cathepsin K is secreted under stressed conditions.[30] We did not observe any increase in the amount of secreted cathepsin in the culture medium from stressed cultures that could explain the absence of higher levels of the intracellular enzyme (data not shown).

Cathepsin activities in cellular extracts from cultures of porcine TM cells grown in a 5% or 40% O_2 environment were quantified using the omnicathepsins fluorogenic substrate Z-Phe-Arg-AMC·HCl. As shown in Figure 6D, incubation of porcine TM cells at 40% O_2 environment did not result in increased lysosomal hydrolytic activity regardless of the increased lysosomal mass. Cell cultures treated with leupeptin showed an increased capacity of hydrolyzing the substrate Z-FR-AMC. This phenomenon has been described in other cell types when repetitive low-dosage of the inhibitor was used.[31]

Discussion

We describe for the first time impaired lysosomal activity in porcine TM cells subjected to chronic oxidative stress. These data represent the first work conducted to determine the correlation of the age-induced decline in lysosomal function with the phenotypic changes observed in the outflow pathway from POAG donors. Also, the data presented in this manuscript clearly validate the use of hyperoxia as an in vitro experimental model to investigate the molecular mechanisms accompanying aging of TM cells.

Today, it is commonly accepted that aerobic metabolism plays a central role in the process of aging. As much as 30% to 40% of all proteins may exhibit protein oxidation as part of normal aging.[32,33] In fact, oxidation and aging are concepts commonly interchanged in the literature. It is also well recognized that oxidation has a key role in the development and/or progression of age-related diseases, including POAG.[9–11] Moreover, the role of oxidative stress is even more relevant in the aging process of tissues, such as the outflow pathway, which is characterized by a low cell renewal rate.[34] Therefore, to reproduce the physiological conditions to which aging TM is exposed in vivo, we selected an experimental model of chronic oxidative stress based on culturing confluent monolayers of porcine TM cells in a high-oxygen environment. This model has been successfully used in similar studies in different cell types, in particular those involving aging of postmitotic cells.[35–38] An important advantage of this model is that because of its relatively low toxicity—no cell death was observed in the stressed cultures—sustained confluence and thus normal post-mitotic conditions were assured throughout the length of the experiment.

As expected, cultures exposed to a 40% O_2 atmosphere demonstrated an increase in intracellular ROS production, decreased Ψm, increased DNA damage, and increased carbonylated proteins, all well-known indicators of oxidative damage. The stressed cells were also characterized by lower proliferation rate, enlarged size, and the accumulation of autofluorescent granules in the perinuclear region. Tripathi et al.[39,40] have described similar morphologic changes in a replicative model of aging in porcine TM cells and in the cells from aged trabecular endothelium, suggesting that such a phenotype might be a common characteristic of aged TM cells. Furthermore, oxidatively stressed cultures demonstrated increased cellular autofluorescence, which is a measure of the lipofuscin content. Lipofuscin, also known as “age pigment,” represents nondegradable material primarily composed of oxidatively modified protein and lipid degradation residues that accumulate and become oxidized within secondary lysosomes.[41] Lipofuscin accumulation is primarily observed in aging postmitotic or terminally differentiated cells, such as neurons, cardiac myocytes, skeletal muscle fibers, and RPE cells.[4]

When observed by TEM, the most striking feature in the cells exposed to an oxidative environment was the increased presence of cytoplasmic membrane-bound organelles containing an electron dense and membranous material. Such organelles were also larger in size than the ones found in the nonstressed cultures (500 nm vs. 200 nm), which were more translucent and contained almost no material. In addition, the cytosol in the stressed cells showed an electron-dense punctate or granular pattern similar to that in some of the membrane-bound organelles. Altogether, their subcellular location, spherical morphology, and the luminal presence of what appears to be material of cytoplasmic origin suggest that such structures are related to the lysosomal cellular pathway. Accordingly, these perinuclear granules were positively stained with the lysosomotropic dyes LTR and AO. Also, flow cytometry quantification analysis confirmed a dramatic increase in lysosomal content in the stressed cultures. These data are consistent with other studies showing that lysosomes of long-lived postmitotic cells become more abundant, larger, and more lipofuscin-loaded with age.[35–38]

The lysosomal compartment is the cellular proteolytic system responsible for the degradation of endogenous and exogenous long-lived proteins, as well as “worn-out” organelles. It is composed of a system of vacuoles that fuse with each other to exchange their contained material. Substrates to be degraded are delivered to the lysosomes via autophagy, a process involving the formation of AVs. These nascent AVs apparently undergo biochemical and morphologic changes (maturation), acquiring lysosomal membrane proteins and hydrolases that subsequently allow them to degrade the sequestered

substrates (autophagolysosomes). In vivo labeling with MDC corroborated augmented AV/autophagolysosome content in the stressed cultures.

All the evidence indicates that TM cells efficiently respond to the presence of oxidative damage by activating the lysosomal degradative pathway, as manifested by the increased presence of novel lysosomes and AVs. A similar response, although to a much lesser degree, was observed in chronic protease inhibition conditions with leupeptin treatment. In addition, protease inhibition induced only a slightly synergistic response when combined with oxidative damage. These findings suggest that it is the peroxidation of the intralysosomal material and not just the accumulation of material within lysosomes, per se, that leads to the acquisition of aging phenotype in TM cells.

Our laboratory has recently reported an increased number of cells positively stained for SA-β-galactosidase in the outflow pathway from glaucomatous donors compared with age-matched control cellss.[12] An interesting finding was that leupeptin-treated and oxidatively stressed cultures showed elevated SA-β-gal activity. The effect was even more pronounced when both conditions were combined and followed a pattern similar to the one observed with MDC staining. The increased SA-β-gal activity was probably not due to a significant transcriptional activation of the gene. Although elevated mRNA levels (twofold) were detected in the cultures treated with leupeptin in 40% O_2 conditions, no change at the mRNA levels was observed in leupeptin-treated or oxidatively stressed cultures alone, despite the elevated SA-β-gal activity (50% and 100%, respectively). Our data are in agreement with those in other studies, suggesting that SA-β-gal is a manifestation of residual lysosomal activity at a suboptimal pH, which becomes detectable due to the increase of lysosomal mass and the accumulation of degradative autophagolysosomes loaded with lipofuscin in aged cells.[13–15] Whether the observed increased SA-β-gal activity in the glaucomatous TM tissue is due to an accumulation of lipofuscin-loaded lysosomes remains to be determined.

A variety of age-associated changes in lysosomal hydrolase activities have been reported in the literature, but the alterations seem to vary, depending on the hydrolase assayed and the tissue used. Some studies showed a decrease in lysosomal cysteine protease activity associated with age-related lipofuscin accumulation, but others did not.[27,42–45] In our study, cells treated with leupeptin demonstrated an increase in both protein content and cathepsin activity compared with nontreated cultures. It is likely that such an increase mostly resulted from diminished degradative capacity rather than transcriptional activation, since cathepsin mRNA levels were not significantly affected by leupeptin alone. Cultures exposed to oxidative stress also demonstrated increased cathepsins protein levels. In contrast, mRNA levels seemed to be differentially modulated among specific cathepsins. The most remarkable change was the dramatic upregulation of cathepsin K mRNA (>10-fold). Surprisingly, we did not detect increased intracellular or extracellular protein levels using an antibody specific for cathepsin K. Additional studies are needed to determine whether this result is due to posttranscriptional regulation or to an increased enzyme turnover via autocatalysis or degradation by other endogenous intracellular enzymes.[46]

One of most interesting results found in this study was that despite the increased oxidized material, augmented lysosomal content, and elevated cathepsin protein levels in the cultures grown under 40% O_2, we did not observe increased lysosomal proteolytic activity in these cells. Similar to other proteases, the cathepsins are synthesized as inactive precursors, and are activated by proteolytic removal of the N-terminal propeptide, either by other proteases or by autocatalytic activation at acidic pH in a chain-reaction manner. The processing and activation of lysosomal proteases are tightly regulated events and can be modulated in several ways, including lysosomal pH, propeptides, glycosaminoglycans, endogenous

inhibitors (cystatin family), and oxidation.[47–50] Although we cannot rule out a potential direct effect of ROS on the enzyme structure, the fact that leupeptin-treated cultures grown at 40% O_2 showed elevated cathepsin activity suggests a limited proteolysis, an imbalance between cathepsins and cystatins, or even an inhibitory mechanism resulting from an enzyme-lipofuscin interaction.

Regardless of the specific mechanism, a decline in the degradative capacity within lipofuscin-loaded lysosomes in aging cells will further initiate, as proposed in the “garbage catastrophe theory of aging,” a vicious cycle that can ultimately compromise the cellular recycling processes, thus leading to the accumulation of defective organelles, such as mitochondria or even other components of the proteolytic machinery in aging TM cells.[5,51] For example, the reported decreased proteasome activity in lipofuscin-loaded fibroblasts is believed to result from defective proteasome renewal due to lysosomal failure.[36] Similarly, this decrease may explain the observed proteasome dysfunction in TM cultured cells under chronic oxidative stress and with age.[52,53] In turn, inhibition of the proteasomal function in human TM cells has been shown to induce the accumulation of calpains, the third major cellular proteolytic system, and has been proposed as a potential mechanism favoring the recently reported accumulation of inactive calpain-1 in the glaucomatous TM.[54]

Many types of cells and tissues accumulate oxidatively damaged material during aging and age-related disorders. Example of these oxidation-related diseases in which the lysosomal system seems to play an important role are atherosclerosis, age-related macular degeneration, Alzheimer’s disease, and Huntington’s disease.[25,20,55,56] Lysosomal storage disorders have been linked to the occurrence of glaucoma, supporting the importance of the lysosomal system in the proper outflow pathway functioning.[57–59] Lysosomal enzyme activities have been detected in the human aqueous humor and in the TM tissue and are thought to play a crucial role in tissue remodeling and phagocytic activity.[60,61] Thus, an impairment of the lysosomal function in the TM may have detrimental effects on the overall tissue physiology.

In summary, our results indicate that chronic exposure of TM cells to oxidative stress causes the accumulation of nonde-gradable material within the lysosomal compartment leading to diminished lysosomal activity and increased SA-β-gal expression. Because the lysosomal compartment is responsible for maintaining general cellular turnover, such impaired activity may lead to a progressive decline in the TM cell function and thus contribute to the progression of POAG.

Supplementary Material

Refer to Web version on PubMed Central for supplementary material.

Acknowledgments

The authors thank Ying Hao for excellent technical assistance in the TEM studies, and Thusita R. Dissanayake (Flow Cytometry Facility, Duke University) for extraordinary help in the flow cytometry analyses.

Supported by National Eye Institute Grants NEI EY01894, NEI EY016228, and NEI EY05722, and Research to Prevent Blindness.

References

1. Leske MC, Wu SY, Hennis A, Honkanen R, Nemesure B. Risk factors for incident open-angle glaucoma: the Barbados Eye Studies. Ophthalmology. 2008; 115:85–93. [PubMed: 17629563]
2. Beckman KB, Ames BN. The free radical theory of aging matures. Physiol Rev. 1998; 78:547–581. [PubMed: 9562038]

3. Harman D. Aging: a theory based on free radical and radiation chemistry. J Gerontol. 1956; 11:298–300. [PubMed: 13332224]
4. Grune T, Merker K, Jung T, Sitte N, Davies KJ. Protein oxidation and degradation during postmitotic senescence. Free Radic Biol Med. 2005; 39:1208–1215. [PubMed: 16214036]
5. Terman A, Brunk UT. Oxidative stress, accumulation of biological 'garbage', and aging. Antioxid Redox Signal. 2006; 8:197–204. [PubMed: 16487053]
6. Barja G. Free radicals and aging. Trends Neurosci. 2004; 27:595–600. [PubMed: 15374670]
7. Cadenas E, Davies KJ. Mitochondrial free radical generation, oxidative stress, and aging. Free Radic Biol Med. 2000; 29:222–230. [PubMed: 11035250]
8. Sohal RS. Oxidative stress hypothesis of aging. Free Radic Biol Med. 2002; 33:573–574. [PubMed: 12208342]
9. Green K. Free radicals and aging of anterior segment tissues of the eye: a hypothesis. Ophthalmic Res. 1995; 27(suppl 1):143–149. [PubMed: 8577453]
10. Kumar DM, Agarwal N. Oxidative stress in glaucoma: a burden of evidence. J Glaucoma. 2007; 16:334–343. [PubMed: 17438430]
11. Sacca SC, Izzotti A, Rossi P, Traverso C. Glaucomatous outflow pathway and oxidative stress. Exp Eye Res. 2007; 84:389–399. [PubMed: 17196589]
12. Liton PB, Challa P, Stinnett S, Luna C, Epstein DL, Gonzalez P. Cellular senescence in the glaucomatous outflow pathway. Exp Gerontol. 2005; 40:745–748. [PubMed: 16051457]
13. Gerland LM, Peyrol S, Lallemand C, Branche R, Magaud JP, Ffrench M. Association of increased autophagic inclusions labeled for beta-galactosidase with fibroblastic aging. Exp Gerontol. 2003; 38:887–895. [PubMed: 12915210]
14. Kurz DJ, Decary S, Hong Y, Erusalimsky JD. Senescence-associated (beta)-galactosidase reflects an increase in lysosomal mass during replicative ageing of human endothelial cells. J Cell Sci. 2000; 113:3613–3622. [PubMed: 11017877]
15. Yang NC, Hu ML. The limitations and validities of senescence associated-beta-galactosidase activity as an aging marker for human foreskin fibroblast Hs68 cells. Exp Gerontol. 2005; 40:813–819. [PubMed: 16154306]
16. Cuervo AM, Dice JF. How do intracellular proteolytic systems change with age? Front Biosci. 1998; 3:D25–D43. [PubMed: 9407152]
17. Cuervo AM, Dice JF. When lysosomes get old. Exp Gerontol. 2000; 35:119–131. [PubMed: 10767573]
18. Kiffin R, Bandyopadhyay U, Cuervo AM. Oxidative stress and autophagy. Antioxid Redox Signal. 2006; 8:152–162. [PubMed: 16487049]
19. Szweda PA, Camouse M, Lundberg KC, Oberley TD, Szweda LI. Aging, lipofuscin formation, and free radical-mediated inhibition of cellular proteolytic systems. Ageing Res Rev. 2003; 2:383–405. [PubMed: 14522242]
20. Bahr BA, Bendiske J. The neuropathogenic contributions of lysosomal dysfunction. J Neurochem. 2002; 83:481– 489. [PubMed: 12390510]
21. Barnham KJ, Masters CL, Bush AI. Neurodegenerative diseases and oxidative stress. Nat Rev Drug Discov. 2004; 3:205–214. [PubMed: 15031734]
22. Butler D, Bahr BA. Oxidative stress and lysosomes: CNS-related consequences and implications for lysosomal enhancement strategies and induction of autophagy. Antioxid Redox Signal. 2006; 8:185–196. [PubMed: 16487052]
23. Kaemmerer E, Schutt F, Krohne TU, Holz FG, Kopitz J. Effects of lipid peroxidation-related protein modifications on RPE lysosomal functions and POS phagocytosis. Invest Ophthalmol Vis Sci. 2007; 48:1342–1347. [PubMed: 17325182]
24. Keller JN, Dimayuga E, Chen Q, Thorpe J, Gee J, Ding Q. Autophagy, proteasomes, lipofuscin, and oxidative stress in the aging brain. Int J Biochem Cell Biol. 2004; 36:2376–2391. [PubMed: 15325579]
25. Nixon RA, Mathews PM, Cataldo AM. The neuronal endosomal-lysosomal system in Alzheimer's disease. J Alzheimers Dis. 2001; 3:97–107. [PubMed: 12214078]

26. Shacka JJ, Roth KA, Zhang J. The autophagylysosomal degradation pathway: role in neurodegenerative disease and therapy. Front Biosci. 2008; 13:718–736. [PubMed: 17981582]
27. Ivy GO, Kanai S, Ohta M, et al. Lipofuscin-like substances accumulate rapidly in brain, retina and internal organs with cysteine protease inhibition. Adv Exp Med Biol. 1989; 266:31–45. discussion 45–37. [PubMed: 2486158]
28. Biederbick A, Kern HF, Elsasser HP. Monodansylcadaverine (MDC) is a specific in vivo marker for autophagic vacuoles. Eur J Cell Biol. 1995; 66:3–14. [PubMed: 7750517]
29. Helbig H, Hinz JP, Kellner U, Foerster MH. Oxygen in the anterior chamber of the human eye. Ger J Ophthalmol. 1993; 2:161–164. [PubMed: 8334391]
30. Platt MO, Ankeny RF, Shi GP, et al. Expression of cathepsin K is regulated by shear stress in cultured endothelial cells and is increased in endothelium in human atherosclerosis. Am J Physiol Heart Circ Physiol. 2007; 292:H1479–H1486. [PubMed: 17098827]
31. Salminen A. Effects of the protease inhibitor leupeptin on proteolytic activities and regeneration of mouse skeletal muscles after exercise injuries. Am J Pathol. 1984; 117:64–70. [PubMed: 6385726]
32. Davies KJ. Oxidative stress: the paradox of aerobic life. Biochem Soc Symp. 1995; 61:1–31. [PubMed: 8660387]
33. Sohal RS. Role of oxidative stress and protein oxidation in the aging process. Free Radic Biol Med. 2002; 33:37–44. [PubMed: 12086680]
34. Strehler, VL. Time, Cells, and Aging. New York: Academic Press; 1962.
35. Lu L, Hackett SF, Mincey A, Lai H, Campochiaro PA. Effects of different types of oxidative stress in RPE cells. J Cell Physiol. 2006; 206:119–125. [PubMed: 15965958]
36. Sitte N, Huber M, Grune T, et al. Proteasome inhibition by lipofuscin/ceroid during postmitotic aging of fibroblasts. FASEB J. 2000; 14:1490–1498. [PubMed: 10928983]
37. Terman A, Brunk UT. Ceroid/lipofuscin formation in cultured human fibroblasts: the role of oxidative stress and lysosomal proteolysis. Mech Ageing Dev. 1998; 104:277–291. [PubMed: 9818731]
38. Zheng L, Roberg K, Jerhammar F, Marcusson J, Terman A. Oxidative stress induces intralysosomal accumulation of Alzheimer amyloid beta-protein in cultured neuroblastoma cells. Ann N Y Acad Sci. 2006; 1067:248–251. [PubMed: 16803994]
39. Tripathi BJ, Li T, Li J, Tran L, Tripathi RC. Age-related changes in trabecular cells in vitro. Exp Eye Res. 1997; 64:57–66. [PubMed: 9093021]
40. Tripathi, R.; Tripathi, B. Functional anatomy of the anterior chamber angle. In: Jakobiec, FJ., editor. Ocular Anatomy, Embryology, and Teratology. Philadelphia: Harper and Row; 1982. p. 197-248.
41. Terman A, Brunk UT. Lipofuscin. Int J Biochem Cell Biol. 2004; 36:1400–1404. [PubMed: 15147719]
42. Amano T, Nakanishi H, Kondo T, Tanaka T, Oka M, Yamamoto K. Age-related changes in cellular localization and enzymatic activities of cathepsins B, L and D in the rat trigeminal ganglion neuron. Mech Ageing Dev. 1995; 83:133–141. [PubMed: 8583832]
43. Keppler D, Walter R, Perez C, Sierra F. Increased expression of mature cathepsin B in aging rat liver. Cell Tissue Res. 2000; 302:181–188. [PubMed: 11131129]
44. Nakanishi H, Amano T, Sastradipura DF, et al. Increased expression of cathepsins E and D in neurons of the aged rat brain and their colocalization with lipofuscin and carboxy-terminal fragments of Alzheimer amyloid precursor protein. J Neurochem. 1997; 68:739–749. [PubMed: 9003065]
45. Shamsi FA, Boulton M. Inhibition of RPE lysosomal and antioxidant activity by the age pigment lipofuscin. Invest Ophthalmol Vis Sci. 2001; 42:3041–3046. [PubMed: 11687553]
46. Rieman DJ, McClung HA, Dodds RA, et al. Biosynthesis and processing of cathepsin K in cultured human osteoclasts. Bone. 2001; 28:282–289. [PubMed: 11248658]
47. Ishidoh K, Kominami E. Processing and activation of lysosomal proteinases. Biol Chem. 2002; 383:1827–1831. [PubMed: 12553719]
48. Mohamed MM, Sloane BF. Cysteine cathepsins: multifunctional enzymes in cancer. Nat Rev Cancer. 2006; 6:764–775. [PubMed: 16990854]

49. Turk B, Turk D, Turk V. Lysosomal cysteine proteases: more than scavengers. Biochim Biophys Acta. 2000; 1477:98–111. [PubMed: 10708852]
50. Turk V, Turk B, Turk D. Lysosomal cysteine proteases: facts and opportunities. EMBO J. 2001; 20:4629– 4633. [PubMed: 11532926]
51. Hirsch HR. The waste-product theory of aging: waste dilution by cell division. Mech Ageing Dev. 1978; 8:51–62. [PubMed: 692175]
52. Caballero M, Liton PB, Challa P, Epstein DL, Gonzalez P. Effects of donor age on proteasome activity and senescence in trabecular meshwork cells. Biochem Biophys Res Commun. 2004; 323:1048–1054. [PubMed: 15381105]
53. Caballero M, Liton PB, Epstein DL, Gonzalez P. Proteasome inhibition by chronic oxidative stress in human trabecular meshwork cells. Biochem Biophys Res Commun. 2003; 308:346–352. [PubMed: 12901875]
54. Govindarajan B, Laird J, Salomon RG, Bhattacharya SK. Isolevuglandin-modified proteins, including elevated levels of inactive calpain-1, accumulate in glaucomatous trabecular meshwork. Biochemistry. 2008; 47:817– 825. [PubMed: 18085799]
55. Jerome WG. Advanced atherosclerotic foam cell formation has features of an acquired lysosomal storage disorder. Rejuvenation Res. 2006; 9:245–255. [PubMed: 16706652]
56. Bergmann M, Schutt F, Holz FG, Kopitz J. Inhibition of the ATP-driven proton pump in RPE lysosomes by the major lipofuscin fluorophore A2-E may contribute to the pathogenesis of age-related macular degeneration. FASEB J. 2004; 18:562–564. [PubMed: 14715704]
57. Ashworth JL, Biswas S, Wraith E, Lloyd IC. Mucopolysaccharidoses and the eye. Surv Ophthalmol. 2006; 51:1–17. [PubMed: 16414358]
58. Cahane M, Treister G, Abraham FA, Melamed S. Glaucoma in siblings with Morquio syndrome. Br J Ophthalmol. 1990; 74:382–383. [PubMed: 2116163]
59. Cantor LB, Disseler JA, Wilson FM 2nd. Glaucoma in the Maroteaux-Lamy syndrome. Am J Ophthalmol. 1989; 108:426– 430. [PubMed: 2508477]
60. Sawaguchi S, Yue BY, Kawa JE, Chang IL, Twining SS, Meberg B. Lysosomal enzyme and inhibitor levels in the human trabecular meshwork. Invest Ophthalmol Vis Sci. 1994; 35:251–261. [PubMed: 8300353]
61. Weinreb RN, Jeng S, Miller AL. Lysosomal enzyme activity in human aqueous humor. Clin Chim Acta. 1991; 199:1–5. [PubMed: 1834372]

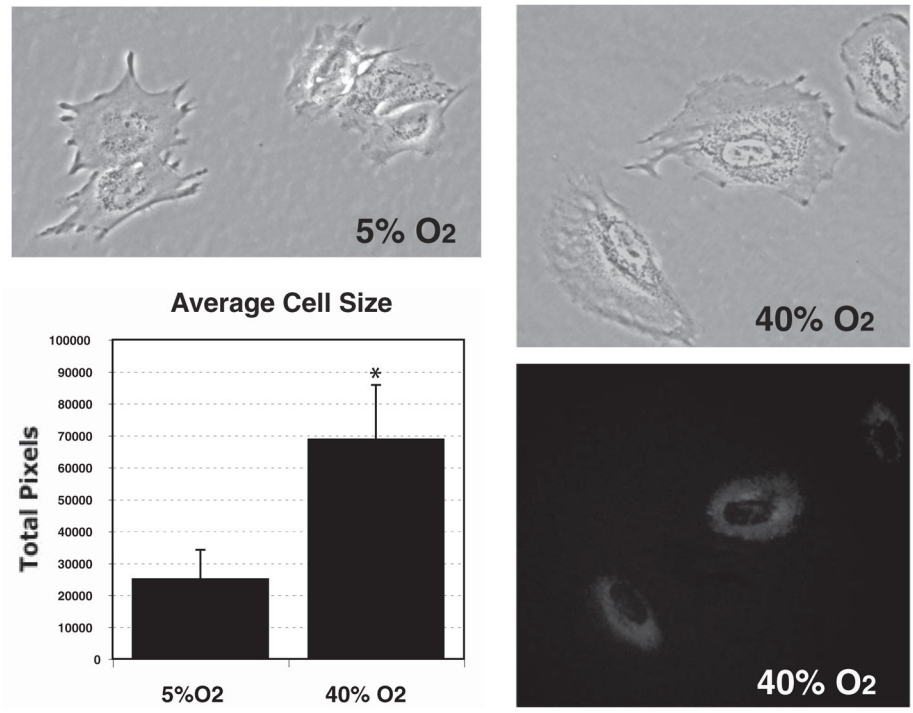

Figure 1.

Morphology of porcine TM cells grown for 2 weeks in physiological (5% O_2) or hyperoxic (40% O_2) conditions. For size measurement purpose, the cells were trypsinized and plated at low density. Images were obtained the following day, and the total number of pixels per cell was quantified. Cells grown at 40% O_2 displayed enlarged size (24,973 ± 9,242 pixels vs. 68,740 ± 17,065 pixels, $n = 20$, $*P < 0.0003$), and exhibited autofluorescent granules in the perinuclear region.

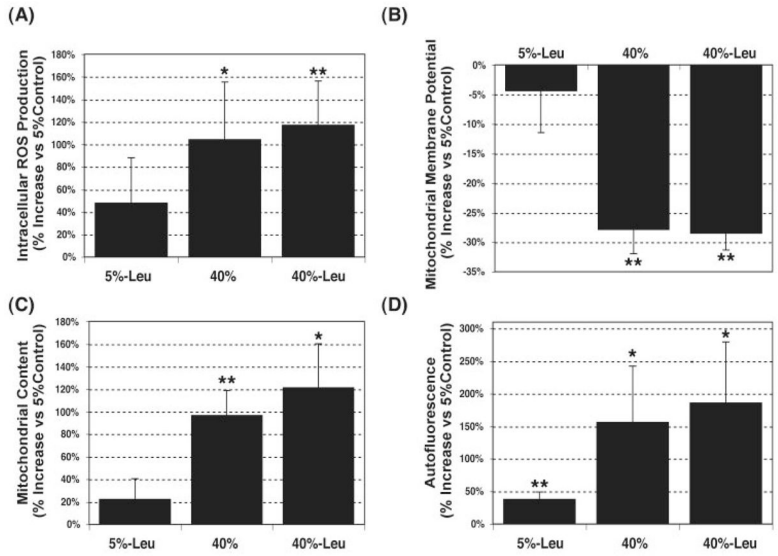

Figure 2.

Oxidative markers in porcine TM cells grown under hyperoxic conditions. Confluent cultures of porcine TM cells were cultured for 2 weeks in 5% or 40% O_2 in the presence or absence of leupeptin (10 μM). Intracellular ROS production (**A**), Ψm (**B**), and mitochondrial cellular content (**C**) were quantified by flow cytometry using the fluorogenic substrates H_2DCFDA, JC-1, and MTR, respectively. (**D**) Cross-linked oxidized material (lipofuscin autofluorescence) was quantified by flow cytometry in the yellow-green range of the spectrum (FL2 channel). Graphs represent the percentage of increase compared with 5% O_2 conditions. Data are means ± SD, $n = 3$, $*P < 0.01$, $**P < 0.001$.

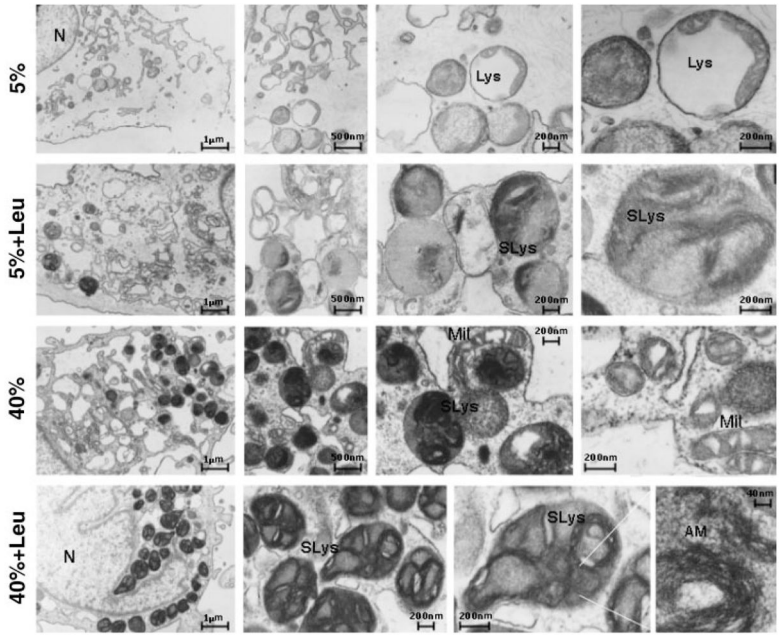

Figure 3.

Ultrastructural appearance of porcine TM cells exposed to chronic oxidative stress in the presence or absence of leupeptin. The cells were detached by scraping, and fixed in 2.5% glutaraldehyde in 0.1 M cacodylate buffer. After fixation, the cells were centrifuged, and the pellet was processed for TEM. Note the appearance in the cultures subjected to oxidative environment of membrane-bound organelles morphologically resembling secondary lysosomes containing an amorphous membranous electron dense material. Lys, primary lysosomes; SLys, secondary lysosomes; Mit, mitochondria; N, nucleus; AM, amorphous material. Data are representative of three independent experiments.

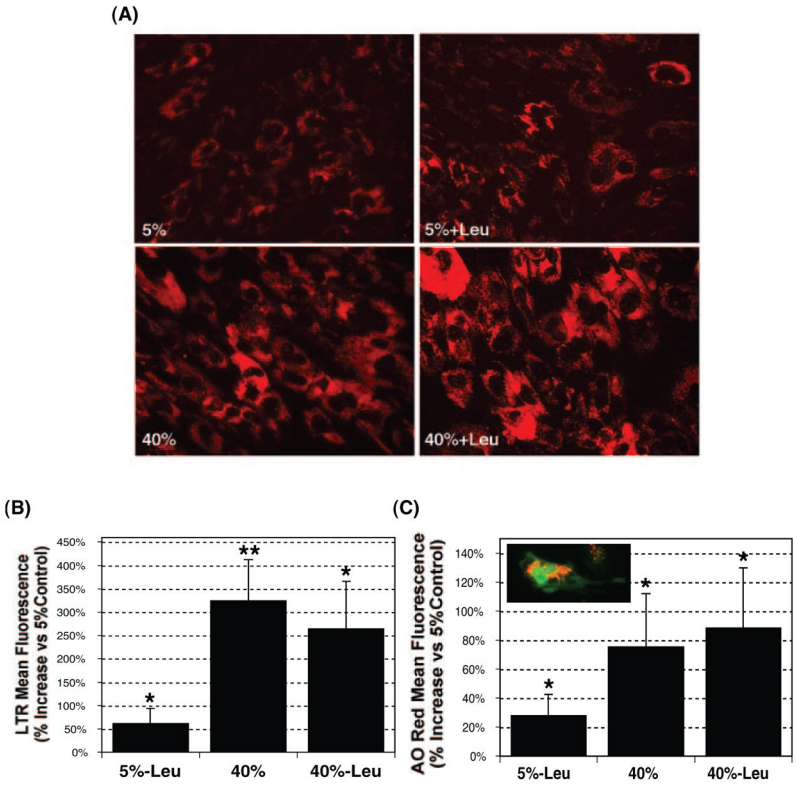

Figure 4.

Effect of oxidative stress and proteolysis inhibition in lysosomal cellular content. After a period of stress, the cultures were loaded with either (**A**, **B**) LTR (500 nM) or (**C**) AO (5 μg/mL) for 15 minutes. Specific lysosomal labeling was confirmed by fluorescence microscopy (**A**, **C**) and quantified by flow cytometry in the red spectrum (**B**, **C**). Observe the perinuclear punctuate red staining in the LTR-loaded cells (**A**) and the lysosome-specific orange staining in the AO-loaded cells (**C**). Graphs represent the percentage of increase compared with 5% O_2 conditions. Data are the mean ± SD, $n = 4$, $^*P < 0.01$, $^{**}P < 0.001$.

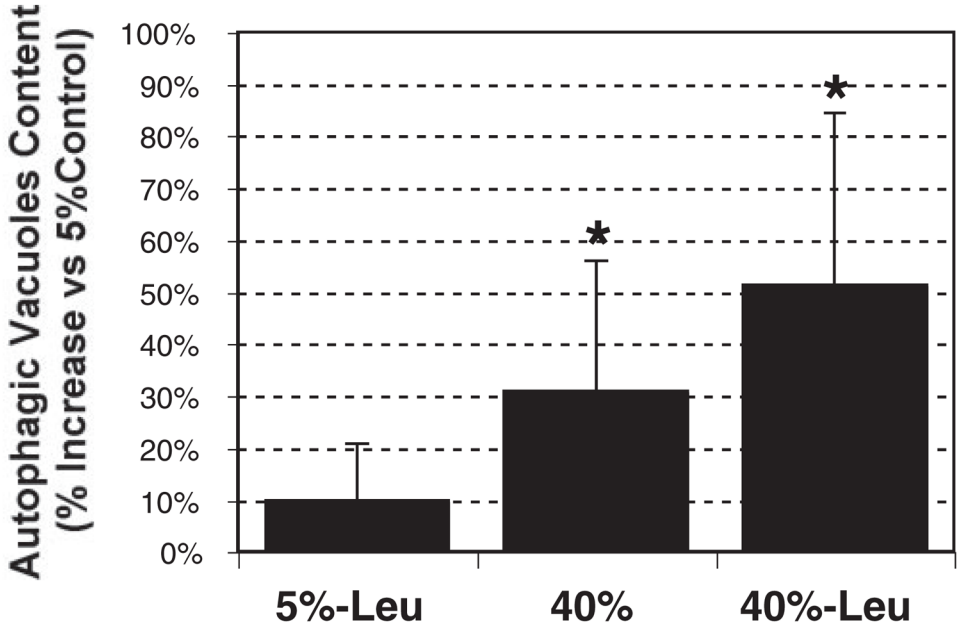

Figure 5.

Effect of oxidative stress and proteolysis inhibition in the AV content: cells were incubated with MDC (0.1 mM) for 15 minutes and lysated, and the AV content was quantified with a microtiter plate reader (exc: 380 nm; em: 530 nm). Ethidium bromide (0.2 μM, exc: 530 nm; em: 590 nm) was used for normalization. Graphs represent the percentage of increase compared with 5% O_2 conditions. Data are the mean ± SD, $n = 6$, $^*P < 0.05$.

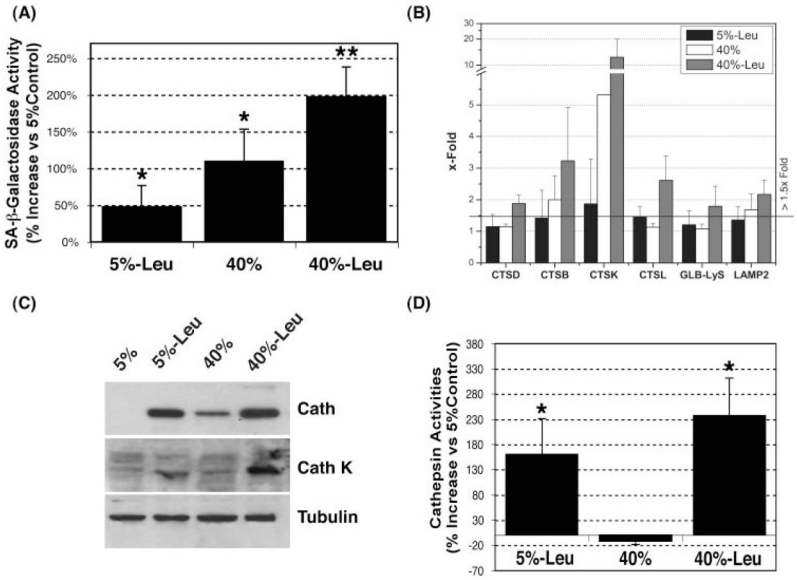

Figure 6.

Analysis of lysosomal function in chronically stressed porcine TM cells: (**A**) SA-β-gal activity was quantified by flow cytometry in chloroquine-treated cells by using the fluorogenic substrate C_{12}FDG. (**B**) Levels of mRNA of several lysosomal cathepsins (CTSD, CTSB, CTSK, and CTSL), GLB-Lys, and LAMP2 were quantified by real-time PCR analysis and normalized with β-actin expression, and the change (x-fold) was calculated compared with the 5% O_2 culture. (**C**) Total cell lysate proteins (20 μg) were separated by SDS-PAGE and immunoblotted with an antibody against a broad spectrum of cathepsins, an antibody against cathepsin K, and anti-tubulin. The results are representative of three independent experiments. (**D**) Lysosomal enzyme activity was determined in cell lysates normalized by total proteins using the omnicathepsin fluorogenic substrate Z-FR-AMC (20 μM). Graphs represent the percentage of increase compared with the 5% O_2 condition. Data are the mean ± SD, $n = 3$, $*P < 0.01$, $**P < 0.001$.

Table 1

Sequence of the Primers Used for qPCR

Description	Unigene	Forward	Reverse
Cathepsin D	CTSD	CAGAAGCTGGTGGACAAGAA	GCGTGACGTTGTGATAGTCC
Cathepsin B	CTSB	GCAACTCCTGGAACACAGAC	CCACGATCTCTGACTCGATG
Cathepsin K	CTSK	ACGTATGAACTGGCCATGAA	ATTACTGCGGGAATGAGAGG
Cathepsin L	CTSL	GGCAAGCTTGTTTCACTGAG	CCTCCATTGTCCTTCACGTA
β-Galactosidase	GLB-Lys	GAGACGTACGTGGCCTGGAAC	TGTAGGGTCCAGGCCTCAGG
LAMP2	LAMP2	TGACTTCGTCTTTGCTGTGA	CATCCCAGTAGCTGAGATTGTT
β-Actin		AAGATCAAGATCATCGCGCCTCCA	TGGAATGCAACTAACAGTCCGCCT